ResearchGate

See discussions, stats, and author profiles for this publication at: https://www.researchgate.net/publication/231675832

Water-Dispersible Tetrablock Copolymer Synthesis, Aggregation, Nanotube Preparation, and Impregnation

ARTICLE *in* LANGMUIR · NOVEMBER 2003

Impact Factor: 4.46 · DOI: 10.1021/la035263w

CITATIONS
60

READS
22

2 AUTHORS:

Zhao Li
National Research Council Canada
45 PUBLICATIONS **1,980** CITATIONS

SEE PROFILE

Guojun Liu
Queen's University
183 PUBLICATIONS **5,996** CITATIONS

SEE PROFILE

Available from: Guojun Liu
Retrieved on: 26 January 2016

Water-Dispersible Tetrablock Copolymer Synthesis, Aggregation, Nanotube Preparation, and Impregnation

Zhao Li and Guojun Liu*

Department of Chemistry, University of Calgary, 2500 University Drive, NW, Calgary, Alberta, Canada T2N 1N4

Received July 11, 2003. In Final Form: September 23, 2003

A tetrablock copolymer polyisoprene-*block*-poly(*tert*-butyl acrylate)-*block*-poly[(2-cinnamoyloxyethyl methacrylate)-*ran*-(2-hydroxyethyl methacrylate)]-*block*-poly(solketal methacrylate), or PI-*b*-P*t*BA-*b*-P(CEMA-*r*-HEMA)-*b*-PSMA, was synthesized and characterized. After PSMA hydrolysis to poly(glyceryl methacrylate), or PGMA, the tetrablock formed cylindrical aggregates in water with a PGMA corona and an insoluble part consisting of PI and P(CEMA-*r*-PHEMA) core−shell cylinders that sandwich a P*t*BA thin layer. Water-dispersible nanotubes were obtained after the cross-linking of the P(CEMA-*r*-HEMA) layer and cleavage of the PI cores with ozone. Both nanotubes containing some ozonized PI fragments and the cross-linked PI-*b*-P*t*BA-*b*-P(CEMA-*r*-HEMA)-*b*-PGMA cylindrical aggregates sorbed Pd^{2+} from dimethylformamide as a result of the π-allyl complex formation between Pd^{2+} and the PI double bonds. The sorbed Pd^{2+} was reduced to Pd nanoparticles, and the particles were made to overlap by catalyzing further Pd deposition on them in an electroless Pd plating bath. These polymer/metal hybrid nanofibers with conductive cores may be useful as nanocables or as a catalyst for reagents that can permeate the P(CEMA-*r*-PHEMA) layer.

I. Introduction

The composition of block copolymers can be tuned to effect the formation of micelles or aggregates of shapes other than spheres in block-selective solvents, as demonstrated by the seminal work of Eisenberg and coworkers[1] and also that of others.[2−7] Block copolymer micelles, which are thermodynamically stable under a given set of conditions, or aggregates, which can be of either thermodynamic or kinetic stability, have many potential applications. They have, for example, been used as templates to produce metal nanoparticles.[8] They are used to pattern surfaces as latent nanoelectronic components[9] or information storage bits.[10] They have also been chemically processed to yield permanent nanostructures[11] including nanospheres,[12−15] shell-cross-linked nanospheres,[16−18] star polymers,[19] hollow nanospheres,[20,21] shaved nanospheres,[22] nanofibers,[23−25] and nanotubes.[26] Mainly diblock copolymers and occasionally triblock copolymers have been used to produce micelles in the past. In this paper, we report on the preparation and characterization of a tetrablock copolymer polyisoprene-*block*-poly(*tert*-butyl acrylate)-*block*-poly[(2-cinnamoyloxyethyl methacrylate)-*ran*-(2-hydroxyethyl methacrylate)]-*block*-poly(glyceryl methacrylate), PI-*b*-P*t*BA-*b*-P(CEMA-*r*-HEMA)-*b*-PGMA. We also report on cylindrical aggregate formation from the polymer in water (A → B, Scheme 1). The aggregates possess a soluble PGMA corona and an insoluble part consisting of PI and P(CEMA-*r*-HEMA) core−shell cylinders that sandwich a thin P*t*BA layer.

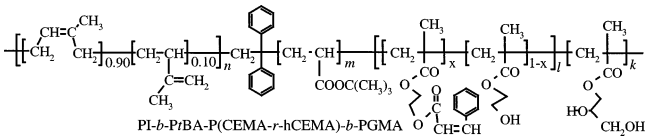

This tetrablock was targeted because the P(CEMA-*r*-HEMA) block could be photo-cross-linked to lock in the cylindrical aggregates to yield nanofibers (B → C). The fibers could then be ozonized to degrade the PI core to yield nanotubes (C → D). Our original plan was to

* Author to whom correspondence should be addressed.

(1) Zhang, L.; Eisenberg, A. *Science* **1995**, *268*, 1728. (b) Zhang, L.; Yu, K.; Eisenberg, A. *Science* **1996**, *272*, 1777. (c) Cameron, N. S.; Corbierre, M. K.; Eisenberg, A. *Can. J. Chem.* **1999**, *77*, 1311.
(2) Ding, J. F.; Liu, G. J.; Yang, M. L. *Polymer* **1997**, *38*, 5497. (b) Ding, J.; Liu, G. J. *Macromolecules* **1977**, *30*, 2408.
(3) Price, C.; Chan, E. K. M.; Hudd, A. L.; Stubbersfield, R. B. *Polym. Commun.* **1986**, *27*, 196.
(4) Jenekhe, S. A.; Chen, X. L. *Science* **1998**, *279*, 1903.
(5) Discher, B. M.; Won, Y.-Y.; Ege, D. S.; Lee, J.C.-M.; Bates, F. S.; Discher, D. E.; Hammer, D. A. *Science* **1999**, *284*, 1143.
(6) Spatz, J. P.; Mössmer, S.; Möller, M. *Angew. Chem., Int. Ed. Engl.* **1996**, *35*, 1510.
(7) Massey, J. A.; Temple, K.; Cao, L.; Rharbi, Y.; Raez, J.; Winnik, M. A.; Manners, I. *J. Am. Chem. Soc.* **2000**, *122*, 11577. (b) Raez, J.; Manners, I.; Winnik, M. A. *J. Am. Chem. Soc.* **2002**, *124*, 10381.
(8) Seregina, M. V.; Bronstein, L. M.; Platonova, O. A.; Chernyshov, D. M.; Valetsky, P. M.; Hartmann, J.; Wenz, E.; Antonietti, M. *Chem. Mater.* **1997**, *9*, 923. (b) Klingelhofer, S.; Heitz, W.; Greiner, A.; Oestreich, S.; Forster, S.; Antonietti, M. *J. Am. Chem. Soc.* **1997**, *119*, 10116. (c) Antonietti, M.; Wenz, E.; Bronstein, L.; Seregina, M. *Adv. Mater.* **1995**, *7*, 1000. (d) Watson, K. J.; Zhu, J.; Nguyen, S. T.; Mirkin, C. A. *J. Am. Chem. Soc.* **1999**, *121*, 462.
(9) Massey, J. A.; Winnik, M. A.; Manners, I.; Chan, V. Z.-H.; Ostermann, J. M.; Enchelmaier, R.; Spatz, J. P.; Möller, M. *J. Am. Chem. Soc.* **2001**, *123*, 3147.
(10) Li, Z.; Zhao, W.; Liu, Y.; Rafailovich, M. H.; Sokolov, J.; Khougaz, K.; Eisenberg, A.; Lennox, R. B.; Krausch, G. *J. Am. Chem. Soc.* **1996**, *118*, 10892. (b) Meiners, J. C.; Elbs, H.; Ritzi, A.; Mlynek, J.; Krausch, G. *J. Appl. Phys.* **1996**, *80*, 2224.
(11) Liu, G. J. *Curr. Opin. Colloid Interface Sci.* **1998**, *3*, 200.
(12) Wang, G. C.; Henselwood, F.; Liu, G. J. *Langmuir* **1998**, *14*, 1554. (b) Henselwood, F.; Liu, G. J. *Macromolecules* **1997**, *30*, 488.
(13) Ishizu, K.; Onen, A. *J. Polym. Sci.: Polym. Chem. Ed.* **1989**, *27*, 3721. (b) Ishizu, K.; Kuwahara, K. *J. Polym. Sci.: Polym. Chem. Ed.* **1993**, *31*, 661.
(14) Prochazka, K.; Baloch, M. K.; Tuzar, Z. *Makromol. Chem.* **1979**, *180*, 2521.
(15) Wilson, D. J.; Riess, G. *Eur. Polym. J.* **1988**, *24*, 617.
(16) Thurmond, K. B., II; Kowalewski, T.; Wooley, K. L. *J. Am. Chem. Soc.* **1996**, *118*, 7239.
(17) Butun, V.; Lowe, A. B.; Billingham, N. C.; Armes, S. P. *J. Am. Chem. Soc.* **1999**, *121*, 4288. (b) Butun, V.; Wang, X.-S.; de Paz Banez, M. V.; Robinson, K. L.; Billingham, N. C.; Armes, S. P. *Macromolecules* **2000**, *33*, 1.
(18) Ding, J. F.; Liu, G. J. *Macromolecules* **1998**, *31*, 6554.
(19) Guo, A.; Tao, J.; Liu, G. J. *Macromolecules* **1996**, *29*, 2487.

10.1021/la035263w CCC: $25.00 © 2003 American Chemical Society
Published on Web 11/12/2003

Scheme 1. Schematic Illustration of Tetrablock Copolymer Processing

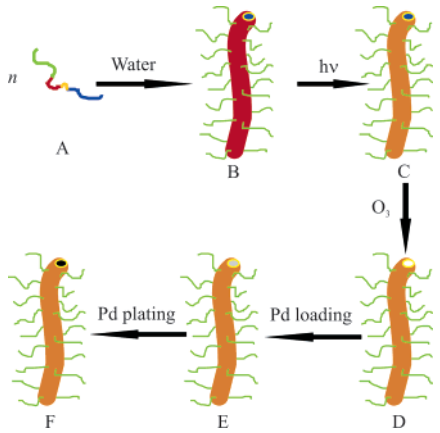

hydrolyze the P*t*BA block next to produce poly(acrylic acid), or PAA, chains on the wall of the inner tube. The PAA groups would bind divalent cations such as Pd^{2+}, which should permeate the cross-linked P(CEMA-*r*-HEMA) layer because of the hydrophilic PHEMA groups. We have since found that this hydrolysis step was unnecessary, because Pd^{2+} could be readily loaded into the core (D → E) if the PI block was not fully ozonized. This happened as a result of π-allyl palladium complex formation between $PdCl_2$ and the residual double bonds of the PI block. After loading and then reducing the loaded Pd^{2+} in the Pd "loading step", we succeeded in depositing more Pd in the cores by electroless plating using a water-born recipe in the "plating step" to yield seemingly overlapping Pd nanoclusters in the cores (E → F). These hybrid fibers with an insulating shell and conductive core may find applications as nanocables[27] or a catalyst for reagents that can permeate the cross-linked P(CEMA-*r*-HEMA) layer.

The nanocables produced here are similar in structure to that of the cylindrical micelles prepared by Massey et al.[7a] In their case, the micellar core was made of a semiconducting polyferrocene block and the insulating shell consisted of poly(dimethylsiloxane). Other related structures include polymer-coated metal nanorods,[28] polymer-coated semiconductor nanorods,[29] and poly(pyrrole)/poly(methyl methacrylate) core−shell fibers produced inside mesoporous silica nanochannels.[30]

II. Experimental Section

Reagents. Cyclohexane was refluxed with freshly cut potassium overnight before distillation. Tetrahydrofuran (THF) was dried by refluxing with potassium and a small amount of benzophenone until a deep purple color developed before distillation. Isoprene was stirred with calcium hydride for 0.5 h and then distilled. It was distilled again after the addition of *n*-butyllithium immediately before use. Solketal methacrylate (SMA) was prepared from reacting solketal with methacryloyl chloride following a literature method.[31] SMA, *tert*-butyl acrylate (*t*BA), and trimethyl silyloxyethyl methacrylate (HEMA-TMS) were distilled over calcium hydride and then in the presence of triethyl aluminum just before polymerization. 1,1-Diphenylethylene (DPE) was vacuum-distilled after the addition of some 1.6 M butyllithium solution in hexanes.

Tetrablock Synthesis. The anionic polymerization was performed in a 1-L three-neck round-bottomed flask using a modified vacuum-line technique.[32] First added to the flask was LiCl, at 5 molar equivalents relative to the initiator *sec*-butyllithium to be added later. The flask was flamed, evacuated, and purged with high-purity argon. This process was repeated three times before dry cyclohexane was distilled into the flask and a drop of styrene was added. The styrene monomer was then titrated at room temperature with 1.3 M *sec*-butyllithium in hexane until a yellow color just developed and remained stable for 10 min. At this stage, the required amount of *sec*-butyllithium was injected. This was followed by the injection of isoprene. Isoprene polymerization was allowed to proceed at 45 °C for 1 day. THF, about 5 times the cyclohexane volume, was then distilled into the polymerization flask. The system was cooled to −78 °C in a dry ice acetone bath, and DPE, in 3 times molar excess relative to the initiator, was added. After 10 min, *t*BA was added and allowed to polymerize for 2 h. The HEMA-TMS and SMA monomers were each polymerized also for 2 h. The polymerization was terminated by the addition of degassed methanol containing a few drops of acetic acid.

The acidic methanol also triggered the cleavage of the trimethyl silyl protective groups in the P(HEMA-TMS) block overnight to poly(2-hydroxyethy methacrylate) or PHEMA. The resultant PI-*b*-P*t*BA-*b*-PHEMA-*b*-PSMA polymer solution was concentrated the next day and precipitated on ice crystals. We typically prepare ∼20 g of polymer from each polymerization using 80 mL of cyclohexane and 400 mL of THF as solvents.

After drying PI-*b*-P*t*BA-*b*-PHEMA-*b*-PSMA under vacuum, the polymer powder was stirred with hexanes for 1 day and centrifuged to remove the supernatant containing extracted PI homopolymer. The extraction was repeated another time before the polymer was dissolved in pyridine. The hydroxyl groups of the PHEMA block were converted into CEMA groups by reaction with cinnamoyl chloride at room temperature. To achieve a CEMA labeling efficiency of 67%, the cinnamoyl chloride to PHEMA hydroxyl group molar ratio used was 0.75:1.00. To achieve full cinnamation, the ratio used was 1.5:1.0. PI-*b*-P*t*BA-*b*-P(CEMA-*r*-HEMA)-*b*-PSMA and PI-*b*-P*t*BA-*b*-PCEMA-*b*-PSMA were purified by precipitation in methanol.

To hydrolyze the PSMA block, PI-*b*-P*t*BA-*b*-P(CEMA-*r*-HEMA)-*b*-PSMA, 0.70 g, was dissolved in 20 mL of THF, and 4 mL of 6 M HCl was then added. This solution was stirred for 2 h at room temperature and purified by dialysis against methanol in a tube with a molar mass cutoff of 12 000−14 000 g/mol (Spectro/Pro). The solution was then concentrated and added to diethyl ether to precipitate the polymer. To check the selectivity of the above hydrolysis conditions, we have also subjected PSMA (size exclusion chromatography, or SEC, $M_n = 6000$ g/mol and $M_w/M_n = 1.05$), P*t*BA ($M_n = 3840$ g/mol and $M_w/M_n = 1.85$), and PCEMA ($M_n = 8580$ g/mol and $M_w/M_n = 1.07$) homopolymers to the same treatment separately and analyzed the polymers treated by NMR spectroscopy.

Polymer Characterization. SEC was performed using THF as the eluant. The Waters HT-4 column used was calibrated using poly(methyl methacrylate) standards. The specific refractive index increment dn_r/dc was measured by a Phoenix Precision instrument. The weight-average molar mass was measured in THF using a light scattering (LS) instrument (Brookhaven model 9025) equipped with a 632.8-nm He−Ne laser.

(20) Ding, J. F.; Liu, G. J. *Chem. Mater.* **1998**, *10*, 537. (b) Ding, J. F.; Liu, G. J. *J. Phys. Chem. B* **1998**, *102*, 6107. (c) Stewart, S.; Liu, G. J. *Chem. Mater.* **1999**, *11*, 1048. (d) Ding, J. F.; Liu, G. J. *Macromolecules* **1997**, *30*, 655.
(21) Huang, H.; Remsen, E. E.; Kowalewski, T.; Wooley, K. L. *J. Am. Chem. Soc.* **1999**, *121*, 3805.
(22) Tao, J.; Liu, G. J.; Ding, J. F.; Yang, M. L. *Macromolecules* **1997**, *30*, 4084.
(23) Tao, J.; Stewart, S.; Liu, G. J.; Yang, M. L. *Macromolecules* **1997**, *30*, 2738.
(24) Won, Y.-Y.; Davis, H. T.; Bates, F. S. *Science* **1999**, *283*, 960.
(25) Templin, M.; Franck, A.; DuChesne, A.; Leist, H.; Zhang, Y. M.; Ulrich, R.; Schadler, V.; Wiesner, U. *Science* **1997**, *278*, 5344.
(26) Stewart, S.; Liu, G. J. *Angew. Chem., Int. Ed.* **2000**, *39*, 340.
(27) For a review article on one-dimensional nanostructures see, for example, Xia, Y. N.; Yang, P. D.; Sun, Y. G.; Wu, Y. Y.; Mayers, B.; Gates, B.; Yin, Y. D.; Kim, F.; Yan, H. Q. *Adv. Mater.* **2003**, *15*, 353.
(28) See, for example, Sun, Y.; Gates, B.; Mayers, B.; Xia, Y. *Nano Lett.* **2002**, *122*, 8581.
(29) See, for example, Xie, Y.; Qiao, Z. P.; Chen, M.; Liu, X. M.; Qian, Y. T. *Adv. Mater.* **1999**, *11*, 1512.
(30) See, for example, Jang, J. S.; Lim, B.; Lee, J.; Hyeon, T. *Chem. Commun.* **2001**, 83.
(31) Mori, H.; Hirao, A.; Nakahama, S. *Macromolecules* **1994**, *27*, 35. (b) Zhang, Z. R.; Liu, G. J.; Bell, S. *Macromolecules* **2000**, *33*, 7877.
(32) Morton, M. *Anionic Polymerization: Principles and Practice*; Academic Press: New York, 1983.

Scheme 2. Tetrablock Precursor Synthesis and P(HEMA-TMS) Hydrolysis

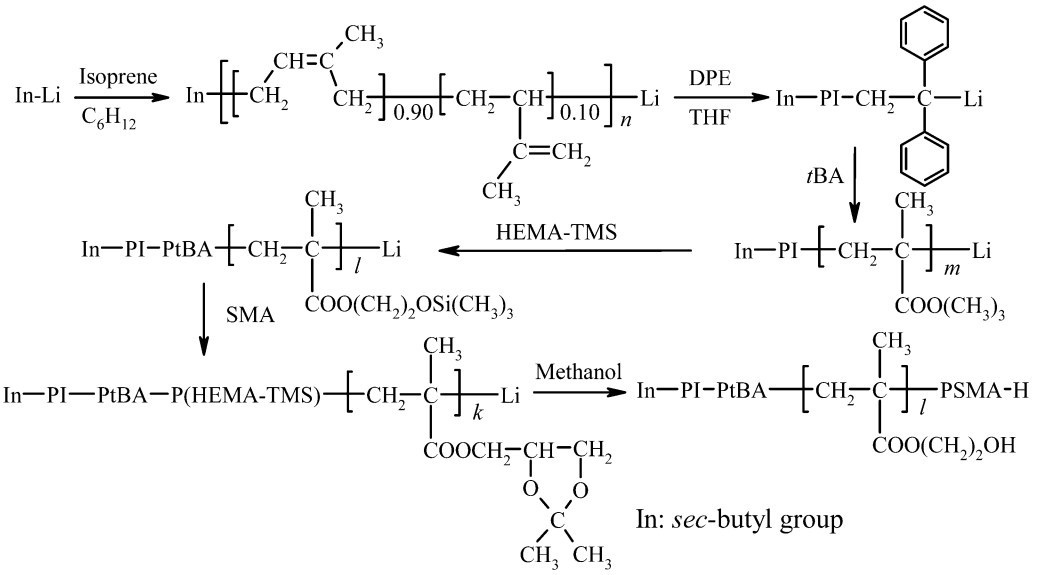

Cylindrical Aggregate Formation and Cross-Linking. Freshly precipitated PI-*b*-P*t*BA-*b*-P(CEMA-*r*-HEMA)-*b*-PGMA, 500 mg, was air-dried in a fumehood for 0.5 h and mixed with 100 mL of distilled water. The mixture was stirred for 4 days, and the resultant milk-like solution was centrifuged at 1550*g* to remove any solid that was not dispersed. The supernatant containing the tetrablock cylindrical aggregates at ~80% yield was irradiated under stirring in a Pyrex round-bottomed flask by a focused UV beam from a 500-W mercury lamp until the CEMA double bond conversion reached 30% as measured by UV spectroscopy.[19]

Ozonolysis. The cross-linked nanofiber solution in water was dialyzed against methanol for solvent switch. The methanol solution at 5 mg/mL was chilled to −78 °C and bubbled with ozone (Welsback generator) until a blue-purple color developed. The solution was stirred further for a pre-designated period, and the excess ozone was purged with nitrogen. Trimethyl phosphite was then added in excess, and the mixture was stirred for 3 h at −78 °C to reduce the ozonides formed. After warming to room temperature, the solution was dialyzed against methanol changed every 12 h or so three times to remove the low-molecular-mass side products.

Palladium Loading. The ozonized nanotubes were precipitated into diethyl ether. The precipitate, 10 mg, after brief drying in a fumehood was redispersed in 10 mL of DMF. This solution was bubbled with argon for 15 min before 15 mg of palladium chloride was added. This yellow solution was stirred overnight and then dialyzed overnight against degassed water changed three times. Pd^{2+} trapped inside the tubular cores was reduced by adding 1 mL of an aqueous $NaBH_4$ solution at 10 mg/mL. The Pd-loaded nanotubes were dialyzed against water to remove reaction side products and impurities.

Palladium Plating. A literature recipe[33] was used to prepare the electroless Pd plating solutions. The Pd salt solution consisted of palladium chloride (78 mg), Na_2EDTA (1.34 g), and saturated aqueous ammonia (7.0 g) in 20 mL of water. The reducing solution consisted of NH_2NH_2 (0.092 mL) in 20 mL of water. The two parts were used always in a 1:2 volume ratio. To plate Pd, Pd-loaded nanotubes or nanofibers in water were mixed with the plating solutions at a given polymer to Pd mass ratio, and the mixture was stirred for a certain time before acetic acid was added to reduce the pH and terminate Pd deposition. The Pd-plated nanotubes or fibers were then dialyzed against water to remove excess agents and impurities.

Transmission Electron Microscopy (TEM). TEM images were obtained using a Hitachi H-7000 instrument operated at 75 kV. To stain the PI double bonds, the nanofibers at 5 mg/mL in water were stirred with $PdCl_2$ at 1.5 mg/mL overnight under an argon atmosphere. The solution was then dialyzed against water to remove excess $PdCl_2$. The PGMA groups were stained by adding a 0.15 M $Ag(NH_3)_2NO_3$ solution slowly into an aqueous nanofiber solution, 5 mg/mL, until a Ag to GMA molar ratio of 1.42:1.00 was reached. The aqueous samples were then aspirated onto a carbon-coated copper grid using a home-built device.[34] To hydrolyze the P*t*BA block, the nanofibers were stirred in a trifluoroacetic acid and dichloromethane mixture (v/v 1:3) for 3 h and then centrifuged.[35] The settled nanofibers were washed with diethyl ether and then redispersed in water. The aqueous solution was aspirated on a carbon-coated copper grid, and the fibers were stained with a drop of a 0.1 wt % uranium acetate, $U(Ac)_2$, solution in ethanol/water (v/v 10:90) for 15 min. The excess staining agent was sucked off with a filter paper placed on the bottom side of the grid and the sample was then rinsed with distilled water. Sample staining by RuO_4 was achieved by exposing a sample aspirated from methanol on a TEM grid to RuO_4 vapor for 4 h.

Thermogravimetric Analysis (TGA). TGA was performed with a Netzch (model STA 449C) instrument. Some 5 mg of the sample was weighed into a sample boat. The sample was then placed along with an empty boat (as a reference) into a furnace that was ramped up to 600 °C at 10 °C/min under a nitrogen atmosphere. The decrease in the sample weight due to polymer decomposition was monitored as a function of the temperature.

Metal content determination in a nanofiber/Pd or nanotube/Pd sample required the analysis of both the precursory nanofiber or nanotube sample and the hybrid sample. Analysis of the precursory sample gives a weight loss fraction of $1 - w_r$ between 150 and 500 °C or a carbonized residual fraction of w_r. The residual fraction w_s of a hybrid sample was assumed to originate from Pd and the carbonized polymer residual. The Pd weight fraction in a sample was calculated using

$$w_{Pd} = \frac{w_s - w_r}{1 - w_r} \tag{1}$$

III. Results and Discussion

Polymer Synthesis. Although the constituent monomers of the tetrablock have been used in different combinations to yield di- and triblock copolymers in our laboratory, the synthesis of a tetrablock has never been attempted before. Scheme 2 shows the reactions invoked to prepare PI-*b*-P*t*BA-*b*-PHEMA-*b*-PSMA. The preparation involved polymerizing isoprene in the nonpolar solvent cyclohexane first to ensure ~90% 1,4-addition.[32] To

(33) Uemiya, S.; Kude, Y.; Sugino, K.; Sato, N.; Satsuda, T.; Kikuchi, E. *Chem. Lett.* **1988**, 1687.

(34) Ding, J. F.; Liu, G. J. *Macromolecules* **1999**, *32*, 8413.

Scheme 3. Tetrablock Derivatization

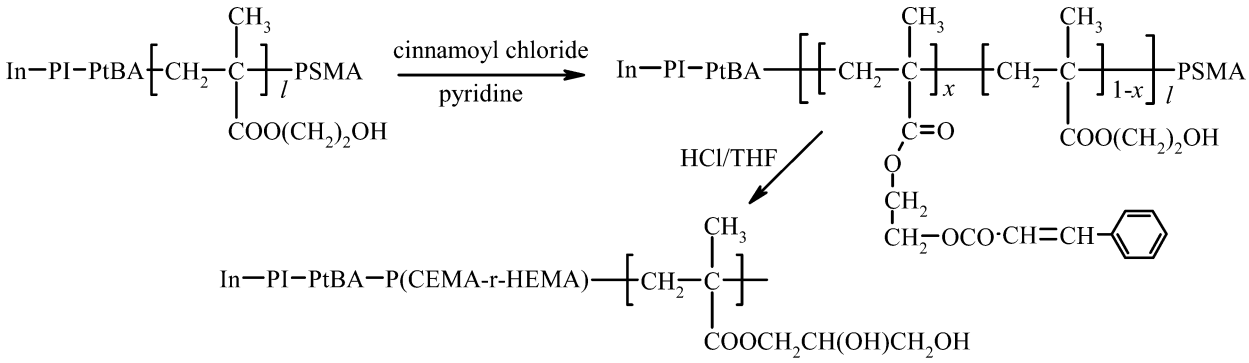

Table 1. Characteristics of PI-*b*-P*t*BA-*b*-P(CEMA-*r*-HEMA)-*b*-PSMA

dn_r/dc (mL/g)	$M_w \times 10^{-4}$ (g/mol) LS	SEC	SEC M_w/M_n	NMR $n/m/l/k$	n	m	l	k	x
0.139	8.2	8.2	1.10	76:5.6:35:100	186	14	86	245	0.67

eliminate impurities in the system before isoprene polymerization, cyclohexane containing a trace amount of styrene was titrated by *sec*-butyllithium until a yellowish color was just observed. Styrene rather than isoprene was used as the indicator for moisture and impurity titration because the polystyrene anions have a much deeper color than the polyisoprene anions. Because the styrene amount used was low, its use should have a negligible effect on the composition and the property of the PI block. After isoprene conversion, the strongly nucleophilic PI terminal anions were reacted with DPE to convert them to the sterically more hindered terminal DPE anions, which helps minimize the *t*BA ester group attack by the anions. THF was introduced into the polymerization flask after isoprene polymerization because methacrylate monomers do not polymerize cleanly in cyclohexane. LiCl was used to reduce the polydispersity of the methacrylate- and acrylate-based blocks. The hydrolysis of P(HEMA-TMS) was achieved by stirring the tetrablock in a THF/methanol mixture containing drops of acetic acid. Further derivatizing reactions are shown in Scheme 3.

Polymer Characterization. Table 1 shows the SEC, ^{1}H NMR, and LS characterization results for the tetrablock PI-*b*-P*t*BA-*b*-P(CEMA-*r*-HEMA)-*b*-PSMA. The ^{1}H NMR spectrum and peak assignments of the tetrablock are shown in Figure 1. Because of peak overlap, it was difficult to determine $n/m/l/k$ and x accurately for PI-*b*-P*t*BA-*b*-P(CEMA-*r*-HEMA)-*b*-PSMA. To eliminate the variable x, we also prepared the tetrablock PI-*b*-P*t*BA-*b*-PCEMA-*b*-PSMA and obtained the ^{1}H NMR spectrum for the sample with the PHEMA block fully cinnamated. Using this sample, the n/l value was determined from the intensity ratio of the PI a peak at 5.1 ppm and PCEMA e peaks between 7.2 and 7.7 ppm or f peaks at ~6.4 ppm. The areas of the e and f peaks were then used to estimate the area of the b peaks of PCEMA between 3.5 and 4.5 ppm, which was subtracted from the total area of the peaks in this region to yield the area for the PSMA c peaks and, thus, $n/l/k$. The area of the *tert*-butyl protons was deconvoluted from that of the acetonide groups of PSMA with the latter calculated from the known area for peaks c of PSMA, which yielded finally $n/m/l/k$. The NMR $n/m/l/k$ ratios agree well with those calculated from the monomer feed ratios. The molar fraction x of CEMA units in the P(CEMA-*r*-HEMA) block was obtained to be 67% from comparing the NMR spectra of PI-*b*-P*t*BA-*b*-PCEMA-*b*-PSMA and PI-*b*-P*t*BA-*b*-P(CEMA-*r*-HEMA)-*b*-PSMA.

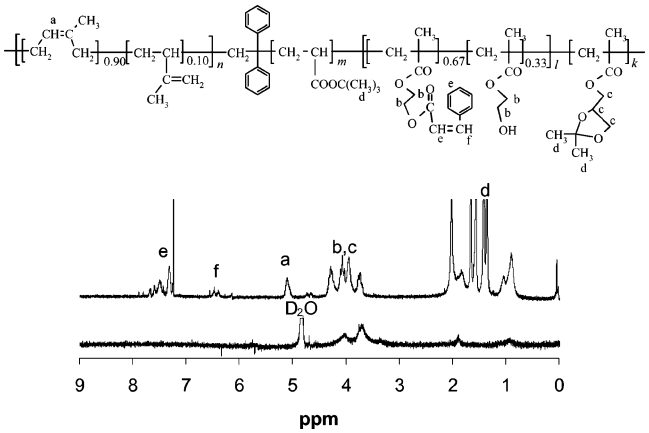

Figure 1. Proton NMR spectra of PI-*b*-P*t*BA-*b*-P(CEMA-*r*-HEMA)-*b*-PSMA in $CDCl_3$ (top) and of PI-*b*-P*t*BA-*b*-P(CEMA-*r*-HEMA)-*b*-PGMA cylinders in D_2O (bottom).

The NMR study of the selective hydrolysis of PSMA under the acidic conditions described in the Experimental Section was made much easier by using the PSMA, P*t*BA, and PCEMA homopolymers, which helped eliminate peak overlap. Under the specified hydrolysis conditions, our NMR results demonstrated that the PSMA homopolymer hydrolyzed quantitatively with no noticeable change to PCEMA and P*t*BA.

Aggregate Formation and Cross-Linking. The PI-*b*-P*t*BA-*b*-P(CEMA-*r*-HEMA)-*b*-PGMA aggregates were prepared by stirring the freshly hydrolyzed tetrablock in water. They were photo-cross-linked before morphological examination by TEM because the cross-linking had been demonstrated before not to perturb aggregate morphology.[23] Figure 2 shows the TEM images of the cross-linked tetrablock aggregates. Images a—c were obtained by staining the sample with RuO_4 vapor. $PdCl_2$, $Ag(NH_3)_2NO_3$, and $U(Ac)_2$ were used as the staining agent to obtain images d—f, respectively. Image a reveals that the aggregates consisted mostly of simple cylinders, which coexisted with some spherical aggregates and branched cylinders. For convenience, the aggregates will be referred to from now on as cylindrical aggregates after the major self-assembly product.

The aggregates could be of kinetic or thermodynamic stability. A thermodynamically stable block copolymer aggregate is formed under a given set of conditions regardless of the production pathway and is called a micelle. We prepared aqueous aggregates of the tetrablock also from dissolving the tetrablock in pyridine molecularly first and then adding water dropwise until the water volume fraction reached 95%. The residual pyridine was removed by dialysis against water. A TEM study revealed that mostly spherical aggregates with a very small fraction

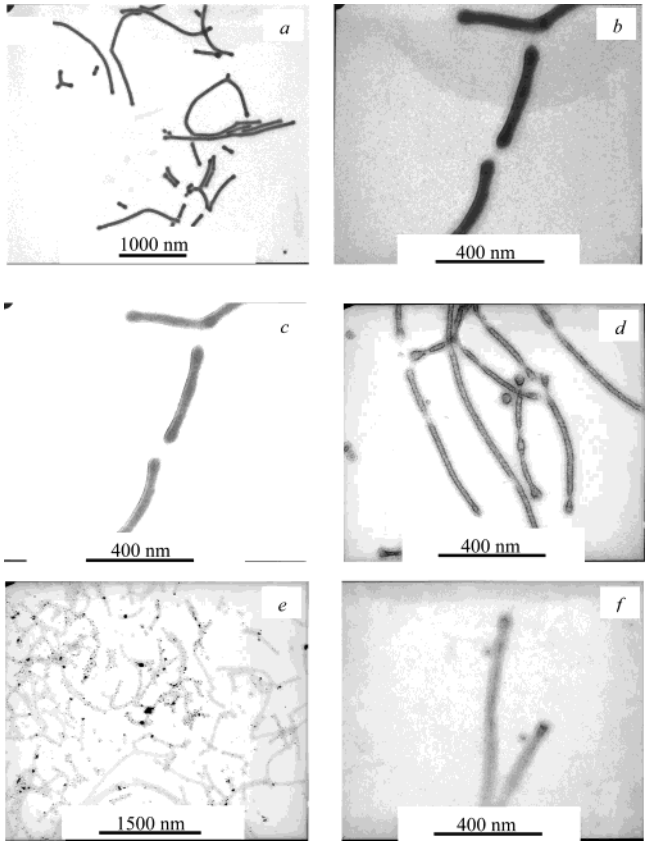

Figure 2. TEM images of cross-linked PI-*b*-P*t*BA-*b*-PCEMA-*b*-PGMA nanofibers stained with RuO_4 (a−c), $PdCl_2$ (d), and $Ag(NH3)_2^+$ (e). Image f was obtained after hydrolyzing the P*t*BA block of the nanofibers and staining the nanofibers by $U(Ac)_2$.

of short cylinders formed in this case. The path-dependent product formation made the origin of the cylindrical aggregates of Figure 2 unknown. This explains why they have been referred to as cylindrical aggregates.

Layered Structure of the Nanofibers. Images b and c in Figure 2 were scanned from the same negative but with the scanning parameters chosen differently so that the different parts of the cylinders were emphasized. In image b, the PGMA layer is visible as a light orange layer with a diameter of ∼84 nm. The insoluble part with double bonds stained by RuO_4 is dark with a diameter of ∼44 nm. Figure 2c emphasizes the contrast inside the insoluble part. The insoluble part appears to consist of a dark core and a gray shell. PI must comprise the darker core, because the density of double bonds that could be stained there was higher than that in the P(CEMA-*r*-HEMA) layer.

To determine the location of the PI block unambiguously, we also tried nanofiber staining by $PdCl_2$, a method that we discovered only after we tried to investigate into how the core of a nanofiber after 15 min of ozonolysis took up an abnormal amount of Pd^{2+}. Since then, we have done a literature search[36] and established the following reaction for the system:

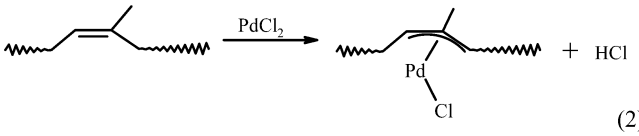

(2)

Thus, the Pd^{2+} uptake was attributed to reaction between the residual double bonds and $PdCl_2$. Figure 2d shows a TEM image of the nanofibers after $PdCl_2$ staining. Only the outer layer of the PI block was stained probably for the short time used to equilibrate the nanofibers with $PdCl_2$. The P(CEMA-*r*-HEMA) block was not stained because it did not contain α hydrogen atoms or the allyl constituent. From this image, the diameter of the PI block is ∼20 nm.

To stain the PGMA block selectively, we took advantage of the fact that vicinal diols reduced $Ag(NH_3)_2^+$.[28] Image e was obtained after aspirating an aqueous nanofiber solution that was reacted with $Ag(NH_3)_2NO_3$. $Ag(NH_3)_2^+$ has evidently been reduced to Ag nanoparticles trapped in the PGMA layer. Thus, this reaction, if optimized, may be used to produce surface-coated polymer/metal hybrid nanofibers.[37]

Further evidence to confirm corona formation from PGMA was provided by a ^1H NMR study of the aggregates formed in D_2O (Figure 1). Proton signals are not seen from any other blocks but PGMA because the other blocks are insoluble and aggregated. The chains in the aggregated part are less mobile, and their signals are flattened out as a result of excessive peak broadening.

The P*t*BA block is short and may not form a distinct phase. The fact that P(CEMA-*r*-HEMA) and PI formed shell−core cylinders suggests that P*t*BA must be located at the interface of the two blocks. To selectively stain P*t*BA, we hydrolyze this block to yield PAA. PAA was then stained with $U(Ac)_2$ to yield Figure 2f. This image suggests that the PAA dark layer is definitely below the P(CEMA-*r*-HEMA) layer. It seems to form a thin layer sheathing the PI core. Other evidence would be required to know if the P*t*BA block actually forms a distinct phase.

Using the diameter of 44 nm for the insoluble part and the densities of 1.25, 1.02, and 0.91 g/cm^3 for PCEMA, P*t*BA, and PI, we could also calculate the diameter for the PI core. This yielded a PI diameter of 29.6 nm, which is larger than the ∼20 nm that we determined directly from $PdCl_2$ staining. The discrepancy might have arisen from the retention or partial retention of the swollen state of the P(CEMA-*r*-HEMA) layer after aspiration from methanol during TEM specimen preparation. The diameter of the aggregate including the PGMA corona from Figure 2b is ∼84 nm. This gives an average PGMA end-to-end distance of 20 nm, which is smaller than the contour length of ∼66 nm for PGMA chains with 245 repeat units but substantially larger than that estimated for PGMA by assuming the unperturbed Gaussian chain conformations. The PGMA chains might be even more stretched in the solvated state. This suggests that PGMA formed a "brush layer" in the corona.[38]

PI Degradation and Nanotube Preparation. PI was decomposed by treating the nanofibers with ozone at −78 °C in methanol. The ozonides formed were then reduced by trimethyl phosphite to yield degraded fragments.[39] Nanotubes were generated only if the PI fragments were extracted from the nanotube cores by methanol.

The degradation of the double bonds was followed using Fourier transform infrared (FTIR) spectroscopy. Figure 3 compares the FTIR spectra of the tetrablock nanofibers after ozonolysis in methanol for 0, 20, and 120 min,

(35) See, for example, Li, Z.; Liu, G. J.; Law, S.-J.; Sells, T. *Biomacromolecules* **2002**, *3*, 984.
(36) Tsuji, J. *Palladium Reagents and Catalysts*; Wiley & Sons: Chichester, 1995. (b) Belfiore, L. A.; Das, P.; Bosse, F. *J. Polym. Sci., Part B: Polym. Phys.* **1996**, *34*, 2675.
(37) Braun, E.; Eichen, Y.; Sivan, U.; Ben-Yoseph, G. *Nature* **1998**, *391*, 775.
(38) Milner, S. *Science* **1991**, *251*, 905.
(39) See, for example, Pine, S. H.; Hendrickson, J. B.; Cram, D. J.; Hammond, G. S. *Organic Chemistry*, 4th ed.; McGraw-Hill: New York, 1980.

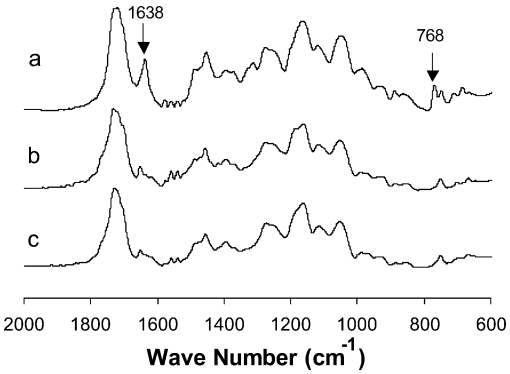

Figure 3. FTIR spectra of PI-*b*-P*t*BA-*b*-P(CEMA-*r*-HEMA)-*b*-PGMA nanofibers at a CEMA conversion of 30% (a) and nanotubes ozonized for 20 min (b) and 2 h (c).

Table 2. TGA Results for the Pd-Impregnated Samples

sample	residual wt % from TGA	Pd wt %
nanotubes	5.78	N/A
Pd-loaded nanotubes	9.56	4.0
Pd-plated nanotubes	23.1	18.4
nanofibers	6.15	N/A
Pd-loaded nanofibers	9.76	3.8
Pd-plated nanofibers	24.8	19.9

respectively. Before FTIR measurements, the fibers were also treated with trimethyl phosphite to reduce the ozonides formed and purified by dialysis against methanol. The double bond absorption peaks at 768 and 1638 cm^{-1} decreased with the ozonolysis time as expected. At 20 min, only a small amount of residual double bonds remained.

PI after full ozonolysis should yield short fragments that can easily permeate the P(CEMA-*r*-HEMA) shell to yield nanotubes. Shell permeability has been demonstrated before for a related system with the loading of a triblock nanotube core by molecules as large as Rhodamine B.[26] We expect formation of fully empty tubular cores, after solvent removal, if the nanofibers are ozonized for more than 2 h and then treated with trimethyl phosphite and extracted by methanol.

Pd^{2+} Loading and Plating. Our original plan was to impregnate the tubular cores with Pd^{2+} via their binding with the carboxyl groups at a molar ratio of 1:2.[40] In demonstrating the permeability of the P(CEMA-*r*-HEMA) shell after PI ozonolysis, we performed a Pd^{2+} loading experiment and discovered that a batch of nanofibers that were ozonized for 15 min uptook a surprisingly large amount of Pd^{2+}. After Pd^{2+} reduction by $NaBH_4$, we determined by TGA analysis 4.0 wt % of Pd inside the hybrid nanofibers (Table 2). This then led to many inquisitive experiments and a literature search to identify the origin of the abnormally high Pd^{2+} uptake. As pointed out before, we have now narrowed down the cause to π-allyl complex formation between Pd^{2+} and the residual PI chain segments that were too long to be extracted out from the nanotube cores after the ozonolysis treatment. This assessment is reasonable because the complex formation reaction has been used to stiffen natural rubber in the past.[36b] Then, the tetrablock nanofibers were able to uptake Pd^{2+} before ozonolysis but failed to do so after ozonolysis was performed to completion using an ozonolysis time of 2 h or more. Therefore, we can control the Pd^{2+} loading amount by adjusting the ozonolysis time and, thus, the double bond concentration inside the nanotube cores, provided that enough time is allowed to reach PI and Pd^{2+} binding equilibrium. Assuming the quantitative reaction between Pd^{2+} and the PI double bonds and the negligible weight change of the nanofiber sample before and after ozonolysis, we, for example, estimated that the particular sample with 4.0 wt % of Pd had a double bond retention rate of ~17% after 15 min of ozonolysis. Thus, the quantification of Pd^{2+} loading may provide a measure of the degree of PI double conversion.

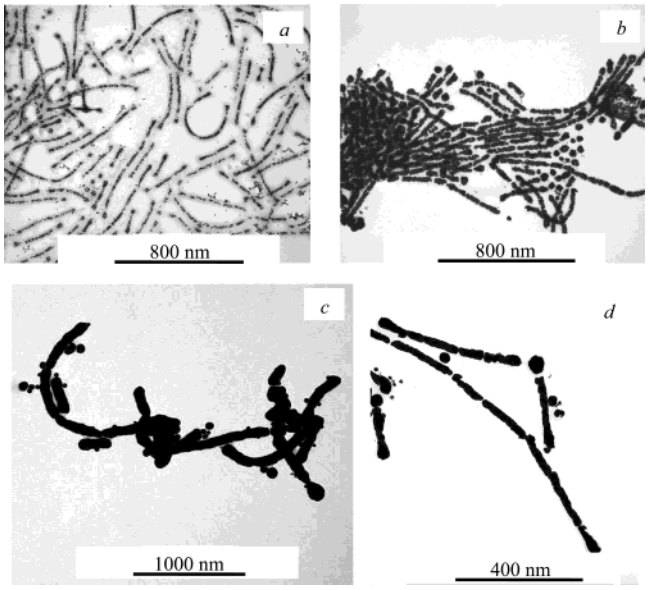

Figure 4. TEM images of polymer/Pd hybrid fibers derived from nanotubes with 4.0 (a), 18.4 (b), and ~39 (c) wt % Pd. Image d shows polymer/Pd hybrid fibers derived from the tetrablock nanofibers with 19.9 wt % Pd.

The complexed Pd^{2+} could be readily reduced by adding $NaBH_4$, as indicated by a sudden color change from yellow-brown to gray. Figure 4a shows a TEM image of the nanotube sample containing 4.0 wt % reduced Pd. The production of Pd under the conditions was anticipated because the reaction had been used by many in the past.[41] The unambiguous evidence for the successful execution of the reaction here is that the Pd loading could be used to catalyze further electroless deposition of Pd using a water-born recipe.

The amount of Pd plated in this step can, in principle, be controlled by adjusting the stoichiometry between Pd^{2+} and nanotubes, provided that sufficient time is allowed for the full deposition of Pd^{2+} from the plating bath. We, for example, calculated from the reaction stoichiometry that a particular sample should have a Pd content of 22.2%. TGA analysis (Table 2) showed the hybrid contained 18.4 wt % Pd. This small difference might be due to the insufficient plating time of 20 min that we used and, thus, the incomplete Pd deposition. Figure 4b shows a TEM image of this sample. The Pd nanoparticles here are larger than those in Figure 4a and seem to form continuous particle strings in certain nanotube cores. Even larger Pd nanoparticles or nanoparticle clusters were prepared by using a higher Pd^{2+} to Pd-loaded nanotube mass ratios. Figure 4c shows a TEM image for a sample with a theoretical Pd weight fraction of 39%. The particles seemed

(40) Lu, Z. H.; Liu, G. J.; Phillips, H.; Hill, J. M.; Chang, J.; Kydd, R. A. *Nano Lett.* **2001**, *1*, 683−687.

(41) See, for example, (a) Boontongking, Y.; Cohen, R. E.; Rubner, M. *Chem. Mater.* **2000**, *12*, 1628. (b) Clay, R. T.; Cohen, R. E. *Supramol. Sci.* **1998**, *5*, 41. (c) Pathak, S.; Greci, M. T.; Kwong, R. C.; Mercado, K.; Prakash, G. K. S.; Olah, G. A.; Thompson, M. E. *Chem. Mater.* **2000**, *12*, 1985.

to have overgrown the core. Impregnating more Pd into each nanotube leads to eventual hybrid nanofiber precipitation.

PI-*b*-P*t*BA-*b*-P(CEMA-*r*-HEMA)-*b*-PGMA nanofibers also sorbed Pd^{2+}. After Pd^{2+} reduction, we plated Pd into the PI-containing cores. Figure 4d shows a TEM image of the nanofibers after Pd plating. TGA yielded a Pd content of 19.9 wt % for this sample.

At 18.4 wt %, Pd seems to have filled the core in Figure 4b. The density of Pd is 11.99 g/cm^3, which is much larger than 0.91 g/cm^3 for PI. These suggest that the Pd particles are quite porous and may function as good catalysts. Then, Pd could be plated into the Pd-loaded tetrablock nanofibers as well. PI degradation after Pd plating would enable the production of even more porous Pd nanoparticles. We have also plated nickel[42] electrolessly into the cores of the Pd-loaded nanotubes. Hybrid nanofibers containing Ni and Co should have interesting magnetic properties.[43]

IV. Conclusions

A functional tetrablock copolymer PI-*b*-P*t*BA-*b*-P(CEMA-*r*-HEMA)-*b*-PGMA that facilitated cylindrical aggregate formation in water was synthesized and characterized. The layered structure of the aggregate has been elucidated by TEM using various selective staining methods. The new $Ag(NH_3)_2^+$ and Pd^{2+} methods may find applications in the TEM studies of the complex solid segregation patterns of multiblock copolymers. The staining methods should also be useful for the selective decoration of certain block copolymer domains with metal. We further demonstrated the chemical processing of the cylindrical aggregates into nanofibers and nanotubes. Both the cores of the nanofibers and those of the nanotubes could be loaded with Pd^{2+}, which was then reduced to yield Pd to catalyze the electroless plating of Pd and other metals including Ni. These polymer/metal hybrid nanofibers are solvent-dispersible and may be used as catalysts. Alternatively, they may function as nanocables.[44]

Acknowledgment. The Natural Sciences and Engineering Research Council of Canada is gratefully acknowledged for sponsoring this research.

LA035263W

(42) Catyrla, F.; Molina, F.; Molina-Sabio, M.; Rodriguez-Reinoso, F. *J. Electrochem. Soc.* **1995**, *142*, 4084.

(43) Yan, X. H.; Liu, G. J.; Liu, F. T. *Angew. Chem., Int. Ed.* **2001**, *40*, 3593.

(44) Duan, X. F.; Huang, Y.; Cui, Y.; Wang, J. F.; Lieber, C. M. *Nature* **2001**, *409*, 66. (b) Uang, Y.; Duan, X. F.; Wei, Q. Q.; Lieber, C. M. *Science* **2001**, *291*, 630. (c) Liu, J.; Casavant, M. J.; Cox, M.; Walters, D. A.; Boul, P.; Lu, W.; Rimberg, A. J.; Smith, K. A.; Colbert, D. T.; Smalley, R. E. *Chem. Phys. Lett.* **1999**, *303*, 125.